

***In-Situ* Measurements of Discharge Plasma Characteristics During Thrust Operation of the T6 Gridded Ion Thruster**

IEPC-2009-151

*Presented at the 31st International Electric Propulsion Conference,
University of Michigan • Ann Arbor, Michigan • USA
September 20 – 24, 2009*

M. H. Corbett*
QinetiQ Ltd, Cody Technology Park, Farnborough, GU14 0LX, U.K.

Abstract: The T6 thruster, developed in QinetiQ, is a 22 cm-diameter Kaufman-type gridded ion thruster that can be optimized for long-duration science missions. In order to help achieve an optimal grid set design for the BepiColombo mission, sets of plasma properties were calculated from Langmuir Probe I-V characteristics measured *in-situ* as an ion beam was extracted. Characteristics were taken at varying radial positions inside the discharge chamber, approximately 5 mm to 14 mm behind the screen grid, from the centre of the grid out to the furthestmost apertures, at various thrust levels. Complications with probe geometry, resulted in a more detailed Druyvesteyn analysis technique being used rather than assume a Maxwellian electron energy distribution. In addition the effect of the measurement environment and plasma effects in relation to the probe geometry were considered when interpreting the absolute values of calculated results. The relative electron number density profile varies by approximately a factor of 2 from centre to edge for thrust levels between 75 mN and 145 mN and the plasma potential is in the range 22 V to 25 V

Nomenclature

A_p	=	Langmuir Probe surface area
e	=	electron charge
k	=	Boltzmann constant
I_e	=	electron current
$f_D(\epsilon)$	=	Druyvesteyn electron energy distribution function
$f_M(\epsilon)$	=	Maxwellian electron energy distribution function
m_e	=	electron mass
n_e	=	electron number density
T_e	=	transverse electron temperature
V_{pl}	=	plasma potential
V_L	=	Langmuir Probe voltage
ϵ	=	electron energy

I. Introduction

The T6 thruster has been in development for over 10 years, originating as a scaled-up version of the 10-cm UK-10 (T5) ion thruster^{1,2}. Over recent years the design has matured into a standalone high-thrust range device, capable of being employed on long-duration science missions or for station-keeping activities³. The thruster is capable of

*Propulsion Scientist, Electric Propulsion Group, Aerospace, EMEA, mhcorbett@qinetiq.com

producing thrust in a nominal range of 75 mN to 200 mN, though the behaviour can be tailored to be either that of a continuous throttling range type or a fixed thrust level type.

Two different primary applications have emerged for the T6 in recent years: for use in the Large Platform Mission Project (AlphaBus) program and as the electric propulsion for the ESA-JAXA BepiColombo mission. Both applications use the same thruster though have different system configuration architectures. This paper deals with plasma characterization activities designed to aid the optimization of the T6 performance to meet the needs of the BepiColombo mission, in particular operation for over 6 years in the thrust range 75 mN to 145 mN. As the T6 performance envelope is very large, where different discharge input parameter combinations can result in the same thrust level, an outcome of investigations will be to minimise excessive discharge chamber erosion due to doubly-charged ions, high anode voltages and high plasma densities, and hence improve lifetime.

The investigations take the form of sets of radial scans of the discharge plasma, performed whilst operating at a fixed thrust level within the BepiColombo range. Each scan consists of a set of Langmuir Probe (LP) I-V characteristics (or traces) taken at fixed radial positions relative to central longitudinal axis of the thruster. A number of scans (3 in total) were performed at each thrust level.

II. Experimental Set-Up and Thruster Operation

A. T6 Thruster

The T6 thruster is a 22-cm diameter Kaufman-type gridded thruster, using an internal cathode-anode circuit, enhanced by a variable magnetic field, to produce ionisation of mass flow rate. In Fig 1, there are photographs of a typical thruster and two thrusters operating simultaneously. What separates the BepiColombo T6 design from other QinetiQ ion thrusters, such as the T5, is that the hollow cathode keeper and anode ring are powered by the same supply, rather than having a separate supply for each. This simplifies the propulsion system design.

B. Ground Support Equipment (GSE) and Chamber

The GSE used was a custom-built set of racks containing remotely controlled power supplies and digital multi-meters operating both at a floating potential of 1850 V (for the high voltage components of the thruster) and ground reference potential. For example, the anode, magnet and cathode heater supplies and associated multi-meters operated at high voltage potential; the accelerator grid voltage and neutraliser keeper supplies and associated meters operated at ground reference potential. The beam supply earth was not isolated relative to the rack earth but commoned with it.

The thruster was installed and operated in the Large European Electric Propulsion facility 1 (LEEP1). This is a 4.7 m long test chamber with a maximum diameter of 2.2 m diameter. It can achieve pressure of less than 1×10^{-6} mbar hence is suitable for operation of high powered ion thrusters such as the T6. A viewing port and a mirror upstream of the thrust were used to take photographs when firing. These were then rotated to actual orientation using the thruster and grid design configurations (Fig. 2).

C. Langmuir Probe Assembly

In order to obtain LP traces as the thruster was firing, a custom-built, L-shaped rotating probe was manufactured and assembled. By replicating mountings and fixture characteristics of the thruster, the probe assembly could be integrated with the minimum of modification to the thruster components. Additionally the probe used a redundant heater wire

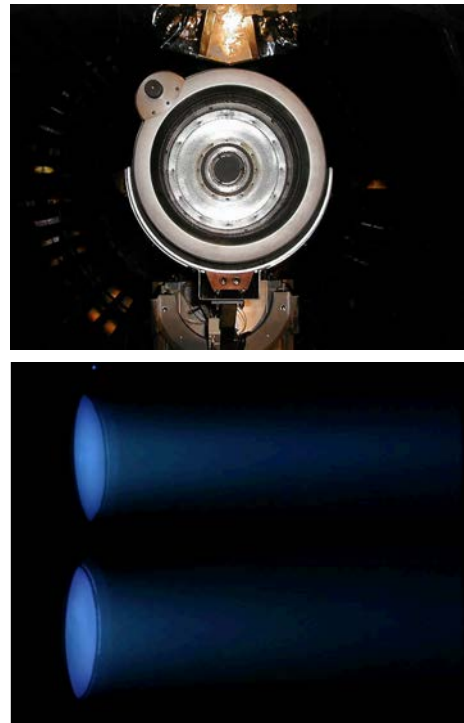


Figure.1 A typical T6 thruster (left) and simultaneous operation of two thrusters (right).

connection for power; hence electrically the probe was invisible to the GSE.

A vacuum-compatible stepper motor was used to drive the probe in an arc of approximately 135° out of a possible 180° defined by physical end-stops on the probe assembly. The arc centre was offset, due to the probe entering the discharge chamber through one of the main gas flow distributor attachment holes, meaning that the scan radius would sample the plasma in an arc from screen grid centre to edge rather than follows a strict radial profile. An assumption in the analysis is therefore that the plasma radial distribution is symmetrical about the axis of the thruster so parameters obtained at each 2-dimensional probe position can be considered to be applicable to a general radial position. The distance of the probe from the screen grid varies by approximately 5 mm to 14 mm.

The motor electronics provided feedback positions as to the number of steps the drive had taken. However, initial investigations showed that this was not adequate to ascertain the probe position to an accurate degree. To achieve this, photographs were taken for each LP trace (Fig. 2). Using photographs taken face on to the grids before integration and the grid aperture configuration, the change in aspect could be accommodated for and the probe position obtained from the photographs.

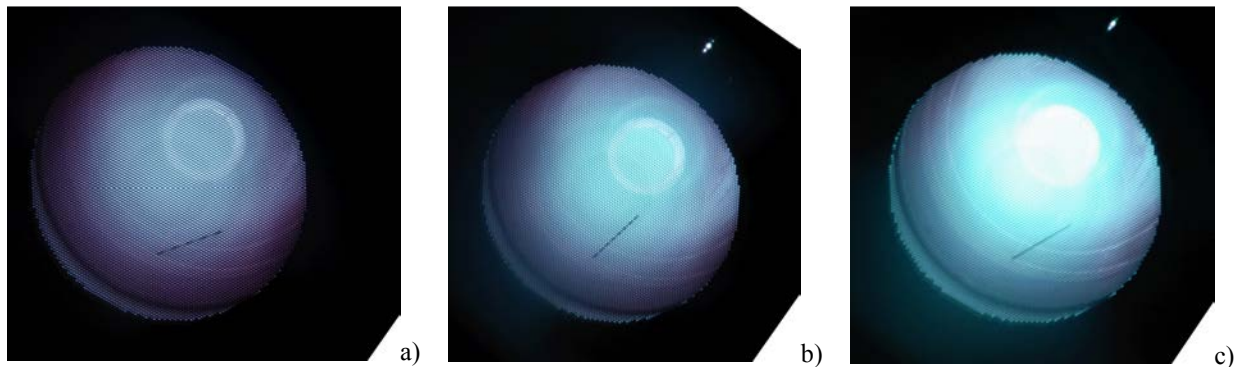


Figure 2. Photographs of the T6 thruster firing during LP testing showing the probe in different positions. The photographs were taken at the following thrust levels a) 75 mN, b) 100 mN and c) 145 mN.

Initial investigations used a cylindrical probe, consisting of an exposed tungsten wire 3.00 ± 0.05 mm in length and 0.35 ± 0.01 mm wide (Surface area = 3.299×10^{-6} m²), at the end of the L-shaped ceramic tube. The voltage range applied was 0 V to 60 V, swept relative to the thruster body potential. The probe voltage would therefore ramp up from discharge body potential through anode potential and then to higher voltages.

This method ran the risk of heating the probe so much, by attracting electrons, that the wire would melt, which is what actually happened after a period of testing. During GSE commissioning for the plasma characterization activities presented in this paper, the probe was observed to glow quite brightly on reaching 60 V. The impression was that the probe wire was being excessively heated. Subsequent scans were then performed between 0 V and 40 V, in an attempt to lessen any heating effect. On opening the chamber after testing and examining the probe, the geometry had become ellipsoid, measuring 0.892 ± 0.05 mm x 0.873 ± 0.05 mm x 0.70 ± 0.05 mm (Surface area = 2.117×10^{-6} m²). As a result of this melting and in order to gain an estimate of plasma parameters with regards to probe geometry effects a Druyvesteyn approach^{4,5} was used in the data analysis. Note that negative voltages were not used and ion current was not investigated in the reported activities, hence all plasma parameters have been estimated by considering the electron branch of the LP trace.

D. Operating Conditions

A set of optimal thruster operating conditions had been determined from previous test campaigns and were applied during the characterization test. The thruster was operated using closed loop control by varying the magnet current to achieve the desired beam current. LP scans were performed at 75 mN, 100 mN, 125 mN and 145 mN once the thruster had been operational for at least an hour. In all conditions the anode voltage was less than 30 V, after correcting for harness impedance (Table 1).

Nominal Thrust	Main Flow Rate	Cathode Flow Rate	Neutraliser Flow Rate	Beam Current	Anode Current	Corrected Anode Voltage
mN	mg/s	mg/s	mg/s	A	A	V
75	1.046	0.691	0.100	1.102	12.19	26.82
100	1.575	0.691	0.100	1.474	14.19	27.83
125	2.083	0.691	0.100	1.844	16.50	28.51
145	2.534	0.691	0.100	2.139	17.99	28.54

Table 1. Thruster operating conditions for LP tests.

III. Langmuir Probe Measurements

A. Probe traces

Twelve sets of radial scans were taken, 3 at each thrust level. The voltage range was 0 V to 40V, with variable voltage steps of 0.5 V over the range 20 V to 30 V, and up to 2 volts elsewhere. The total voltage range was adequate to capture both floating potential and electron saturation regions of the I-V characteristic for all thrust levels (Fig. 3).

The traces all showed increased current noise in the range 30 V to 40 V, which typically would be used to find electron saturation current. However the Druyvesteyn method uses the voltage range up to the plasma potential, which was in the range 22 V to 25 V, so this noise did not present an issue. The floating potential was approximately 2 V to 4 V in all scans and varies in relation to plasma potential. Note that analysis of the floating potential behaviour is limited to the resolution of the voltage range in this portion of the LP trace.

In the analysis, electron current was obtained by removing the estimated ion current. The ion current branch was not fully explored, as negative voltages were not used, so a simplified approach was employed in which the current over 0 V to 2 V was averaged and taken away from the overall probe current. The ion current is not expected to be significantly large so an error in absolute value of electron current was taken as 5%.

Interestingly, even before analysis, the traces in Fig. 3 indicated that there was a reduction in collected current by a factor of 2 at 145 mN between the centre to the grids and the larger radial positions. Position 1 (Pos 1) is at approximately 9 mm from the grid centre; Position 2 is at approximately 90 mm.

B. Electron energy distribution function (EEDF)

The EEDF for each probe trace was calculated by first obtaining the plasma potential from the 2nd derivative. Each LP trace was linearly interpolated to a resolution of 0.1 V, then smoothed with a 25-point moving average, centered on point 13. This reduces the overall voltage range. The 2nd derivative was calculated and plasma potential was obtained from the zero crossing on the voltage axis⁴.

The 2nd derivative was then smoothed again, using another 25-point moving average, centered on point 13, which again reduces the voltage range. A simplified

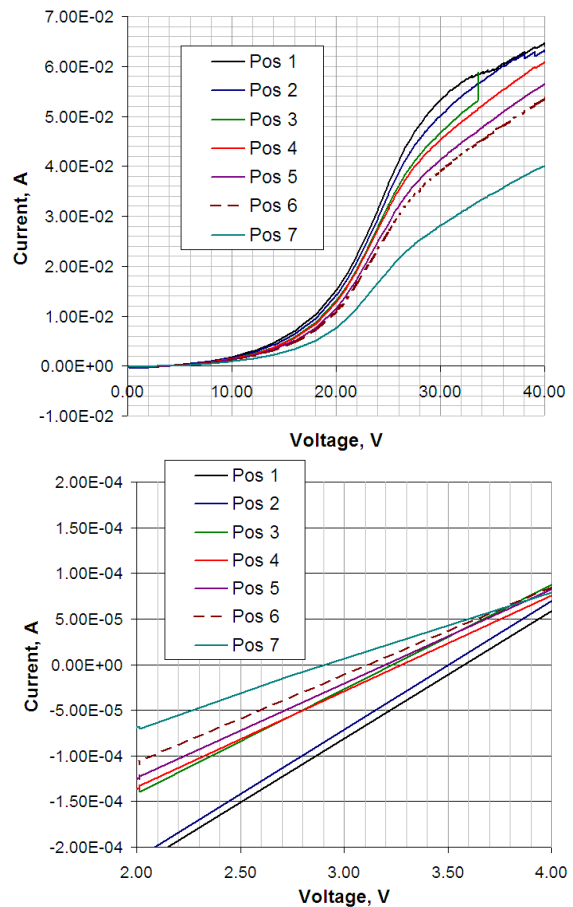


Figure 3 LP traces taken at 145 mN operating conditions. Top shows the traces in their entirety; Bottom shows the floating potential which reduces with increasing radial position.

EEDF was created as an interim measure in lieu of a full EEDF^{5,6} in accordance with Eq. 1. The simplified EEDF is that described within the square brackets of Eq. 1, *i.e.* without the constants. It is used to compare the form of the EEDF calculated with the ellipsoid probe to that with a cylindrical probe without needing to scale the amplitude of the results. Eq. 2 is a Maxwellian using the same formulation⁵.

$$f_D(\varepsilon)_{\varepsilon=-e(V_{pl}-V_L)} = \frac{4}{e^2} \sqrt{\frac{m_e}{2e}} \left[\frac{1}{A_p} \sqrt{(V_{pl}-V_L)} \frac{d^2 I_e}{dV_L^2} \right] \quad (1)$$

$$f_M(\varepsilon)_{\varepsilon=-e(V_{pl}-V_L)} = 2\pi \left(\frac{m_e}{2\pi k T_e} \right)^{\frac{3}{2}} \sqrt{\frac{2e(V_{pl}-V_L)}{m_e}} \exp\left(\frac{-e(V_{pl}-V_L)}{k T_e} \right) \quad (2)$$

Once this simplified EEDF is created, it was smoothed to reduce the saw-tooth artifacts resulting from the original interpolation of the LP trace. The majority of important information was in the lower electron energy range, where the probe voltage is close to the plasma potential; however to estimate number density the high energy tail was extrapolated exponentially, using the fit to the available EEDF information over the highest 5 V range. The associated error in electron number density due to the tail of the EEDF being over-estimated was calculated to be approximately 2% in the worst-case.

Electron number density was calculated by using the statistical sum of the full EEDF over all energies^{5,6} (Eq. 3)

$$n_e = \int_0^{\infty} f(\varepsilon) d\varepsilon \quad (3)$$

. Electron temperature was calculated as the transverse electron temperature (Eq.4), which is the effective electron temperature of the velocity distribution of charges reaching the probe⁶.

$$T_e = \frac{2}{3} \cdot \frac{1}{n_e} \int_0^{\infty} \varepsilon f(\varepsilon) d\varepsilon \quad (4)$$

IV. Analysis Results

A. Comparing the cylindrical EEDF to ellipsoid EEDF

During initial investigations and before the probe melted, LP traces were taken over at what was thought to be a radial profile at the defined thrust levels. However on opening the chamber the probe motion had been compromised, which led to the reliance on taking photographs for each scan to unambiguously confirm the probe was moving and to determine the probe position. By applying the analysis technique to traces taken when the probe was cylindrical and by assuming that the traces, as presented in this paper, were taken with an ellipsoid probe, the simplified EEDF can be compared (Fig. 4). A scaled Maxwellian distribution (with electron temperature of 5 eV) that has the similar area to the EEDF and an EEDF taken under 145 mN discharge conditions have been included.

Both high energy tails of the EEDF appear to be larger than the Maxwellian, though these tails are extrapolated. The cylindrical probe has a lower energy peak than the ellipsoid probe, though both have a similar number density when summed. The radial distance of the cylindrical probe from the centre of the grids could be larger than the

ellipsoid probe (which is known) so the number density of a cylindrical probe, placed in the same position as the ellipsoid could be larger. The calculated EEDF for both probe geometries suggest that the plasma is either non-Maxwellian or anisotropic or both. Anisotropy has been considered for various probe geometries including cylindrical probes^{6,7} while non-Maxwellian distributions have been studied in reference to the Druyvesteyn method⁸. In both instances, the recommendation is to use the EEDF method to calculate electron number density.

Anisotropy could be caused by the probe geometry or it could be an actual plasma phenomenon, in that at this position, close to the grid, with ions being extracted, the plasma is flowing over the probe. The EEDF obtained under discharge conditions has less high energy electrons and a lower energy peak.

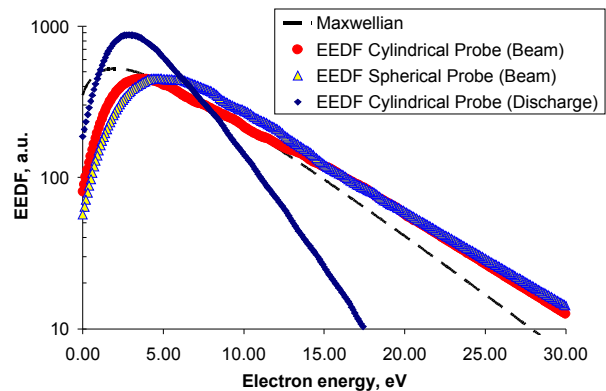


Figure 4 Calculated simplified EEDF for a cylindrical and ellipsoid (near spherical) probe at 145 mN conditions. The ellipsoid EEDF is close to the centre of the grid. A Maxwellian distribution and EEDF obtained under 145 mN discharge conditions are also included.

B. Electron number density, plasma potential and electron temperature

A number of assumptions and error estimated were applied in the calculation of plasma parameters:

- That the Druyvesteyn method is applicable to the plasma conditions and the ellipsoid probe (being nearly spherical⁴)
- That the probe melted sufficiently so that the probe area at the time of measurement is the same as measured afterward
- That the characteristic of the number density rather than the absolute values is correct for the plasma conditions across the grid
- That the errors will be limited to probe area error (2%), EEDF fit error (5%), ion current subtraction (5%) and doubly charged ion content (5%). The total root-sum-squared error for number density is 7.6% and for electron temperature it is 7.8%. A general error of 8% will be used.
- That the errors in plasma potential are 0.2 V due to zero-crossing determination. The plasma potential can be underestimated by using the zero-crossing method⁷ but this will not be explored in this paper.
-

The results (Fig. 5 and Fig. 6) show that the electron number density varies approximately as a quadratic relationship across the radial profile of the grids for all thrust levels investigated. The electron number density varies by factor of 2 approximately, from grid centre to grid edge. The electron temperature is in the range 5.5 eV to 7.0 eV and reduces slightly for increasing radial position for all thrust levels except 75 mN. The plasma potentials are in the range 22 V to 25 V and they vary in the same way as electron temperature across the grid. The electron temperature behaviour at 75 mN is what would be expected if the EEDF was approximately Maxwellian⁴, in that there should be an increase as number density drops, yet the EEDF at this thrust level are non-Maxwellian and are consistent in form to all the EEDF calculated.

There is still doubt as to whether the absolute values of number density and electron temperature are correct and reflect the plasma conditions. The ellipsoid probe, being formed from a melted cylindrical probe, is much shorter in length and the collection area is closer to the ceramic tube. A suggestion is that the effective area of the probe may be less than appears as there is an interaction with the floating sheath around the ceramic tube near the exposed probe. If the effective area was less, this would have the effect of increasing number density and reducing electron temperature, though it should not affect the plasma potential. Plasma simulations performed during T6 optimization have typically used electron temperatures of 3 eV.

The cylindrical probe scan, where one trace was used to create the EEDF in Fig. 4, also resulted in an electron temperature of approximately 5.7 eV, decreasing with apparent increasing radial distance, and a similar number density to the ellipsoid probe using the Druyvesteyn method. As the positional information is more vague when this scan was taken *i.e.* the radial position could be anywhere between 0 mm and 60 mm from the grid centre, it is possible that the number density could be higher in reality, perhaps by a factor of 2.

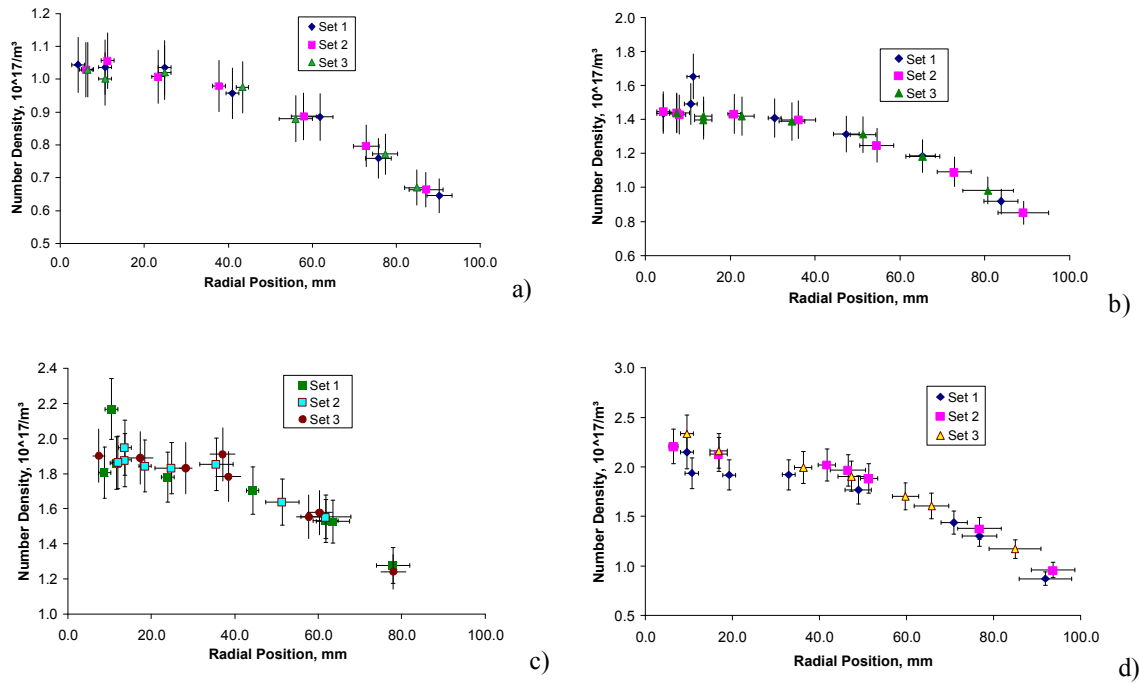


Figure 5 Electron number densities, for thrust levels a) 75 mN b) 100 mN c) 125 mN and d) 145 mN, calculated using the Druyvesteyn method and assuming an ellipsoid geometry as measured afterward.

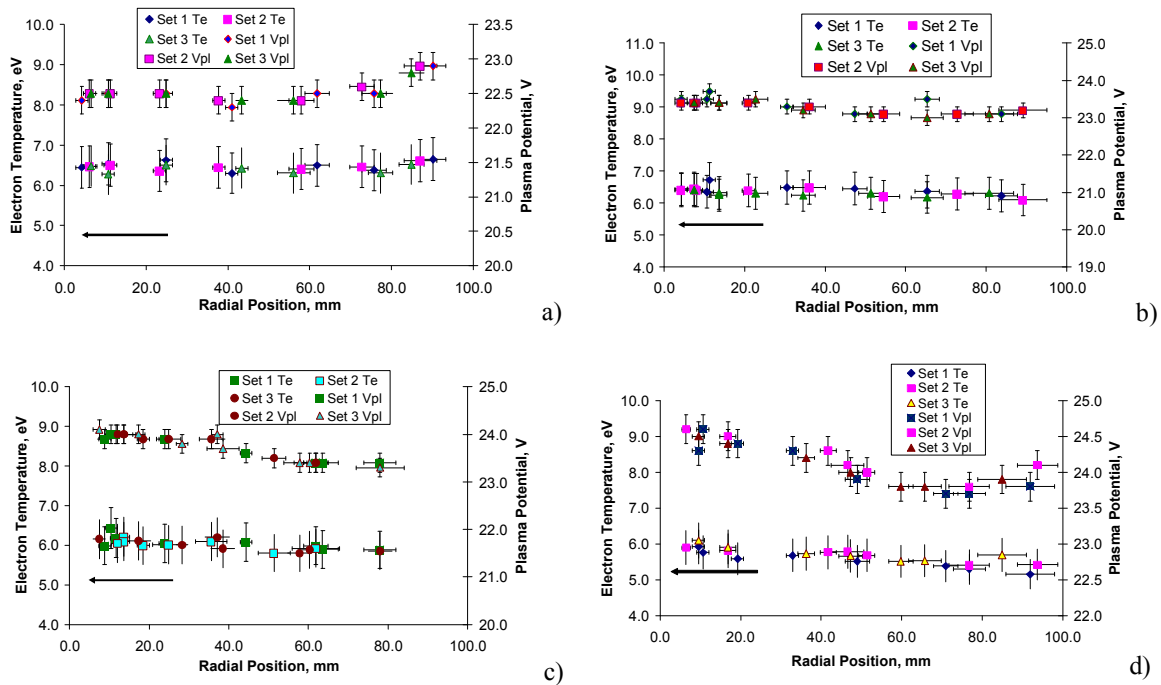


Figure 5 Electron temperatures and plasma potentials, for thrust levels a) 75 mN b) 100 mN c) 125 mN and d) 145 mN, calculated using the Druyvesteyn method and assuming an ellipsoid geometry as measured afterward.

V. Conclusion

Sets of Langmuir Probe traces were taken at various radial positions along the grid profile of the T6 thruster, operating at the thrust levels 75 mN, 100 mN, 125 mN and 145 mN. The data sets were obtained to help in the optimization of the thruster performance for the BepiColombo mission. Some complications arose in the analysis due to the probe geometry in that the probe melted into an ellipsoid from a cylinder during testing. By comparing previous data sets obtained in the same experimental conditions, before the set of tests described in the report were performed, it was possible to bound the calculated plasma parameters to a range of values.

The results thus show that:

- The EEDF appears to be non-Maxwellian and anisotropic for both cylindrical and ellipsoid (near-spherical) probe geometries. The distribution of energies also varies with probe geometry with the cylindrical probe having a lower peak energy. In addition, an EEDF taken under discharge conditions appears to show that the extraction of ions leads to a greater degree of deviation from a Maxwellian distribution.
- The number density profile at all thrust levels tested varies by a factor of 2 approximately, from the grid centre to the edge
- The absolute values of number density at 145 mN are at least $2 \times 10^{17} \text{ m}^{-3}$ at the centre of the grid, and quite possibly twice this value
- Electron temperatures are calculated to be in the range 5.5 eV to 7 eV, with the higher temperature occurring at lower thrust levels.

To try and resolve these issues, further work will be undertaken with cylindrical probes, initially of the same size as the original, with the voltage range increased into the negative voltage region to capture the ion current.

Acknowledgments

M. H. Corbett thanks Orson Sutherland from ESTEC (ESA), Noordwijk, The Netherlands, Stephen Gabriel from Southampton University, U.K. and Dan Goebel, Jet Propulsion Laboratories, Pasadena, California, USA for discussions and input with regards to probe geometry effects on the analysis results.

References

- ¹Fearn, D. G., Martin, A. R. and Smith, P., "Ion Propulsion Research and Development in the UK", *Journal of the British Interplanetary Society*, Vol. 43, 1990, pp 431-442.
- ²Wallace, N. C., Mundy, D. H., Fearn, D. G. and Edwards, C. H., "The UK-10 Ion Propulsion System – a Technology for Improving the Cost-Effectiveness of Communications Spacecraft", *AIAA / ASME / SAE / ASEE 35th Joint Propulsion Conference and Exhibit*, AIAA-99-2442, Washington, D.C., 1999.
- ³Simpson, H. W., Wallace, N. C., Doughty, S. R., Rudwan, I. M. and Corbett M. H., "From Earth to Mercury: QinetiQ's Electric Propulsion Technology", *59th International Astronautical Congress*, IAC-08-D1.1.01, Glasgow, U.K.
- ⁴Lochte-Holtgreven, W., *Plasma Diagnostics*, 1st ed., North-Holland Publishing Company, Amsterdam, 1968, Chap. 11.
- ⁵Monterde, M. P., Haines, M. G., Dangor, A. E., Malik, A. K. and Fearn, D. G., "Kaufman-type xenon ion thruster coupling plasma: Langmuir probe measurements," *Journal of Physics D: Applied Physics*, Vol. 30, No. 5, 1997, pp. 842-855.
- ⁶Sudit, I. D. and Woods, R. C., "A study of the accuracy of various Langmuir Probe theories," *Journal of Applied Physics*, Vol. 76, No. 8, 1994, pp. 4488-4498.
- ⁷Woods, R. C. and Sudit, I. D., "Theory of electron retardation by Langmuir probes in anisotropic plasmas," *Physical Review E*, Vol. 50, No. 3, 1994, pp. 2222-2238.
- ⁸Godyak, V. A., Piejak, R. B. and Alexandrovich, B. M. "Probe diagnostics of non-Maxwellian plasmas," *Journal of Applied Physics*, Vol. 73, No. 8, 1993, pp. 3657-3633.